Assimilation of radar reflectivity for rainfall nowcasting

Yann Lepoittevin, Isabelle Herlin

ASSIMILATION OF RADAR REFLECTIVITY FOR RAINFALL NOWCASTING

Yann Lepoittevin [1] * *Isabelle Herlin* [1]

[1]INRIA, Institut National de Recherche en Informatique et Automatique, France

ABSTRACT

The paper describes an operational method of rainfall nowcasting based on ground radar acquisitions with high space and time resolution. The nowcast horizon is between 30 minutes and 1 hour as required by prevention measures of flash floods. The characteristics of the input data justify the design of an image-based method that estimates wind fields from image acquisitions and forecasts the location and quantity of rain in the near future. The estimation phase relies on an iterative data assimilation of the radar acquisitions with an evolution model of motion and image fields, while the forecast is obtained by simulating these fields at the chosen horizon. The research is done in the context of a collaboration with the french company Numtech and the data are obtained with radars of the company Weather Measures.

***Index Terms*—** Radar image, rain nowcasting, motion estimation, data assimilation.

1. INTRODUCTION

The paper describes an operational method for rainfall nowcasting and prevention of flash floods. The available observation data are rainfall rates, acquired every 5 minutes from ground radars, as displayed on Fig. 1. The operational conditions lead to two major constraints. First, the forecast must be available less than five minutes after data acquisition and updated as soon as a new image is available. This is mandatory for having enough time to apply emergency measures. Second, the forecast must be accurate long enough, at least 30 minutes to 1 hour, so that these emergency measures remain valid. These temporal requirements clearly prevent the use of Numerical Weather Prediction Models (NWP) and force to only rely on radar images as explained in Mecklenburg et al. [1], even if results' quality strongly depends on that of the image acquisitions.

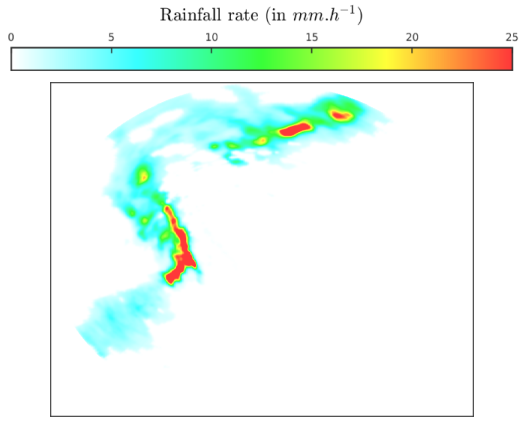

Fig. 1. Rainfall rate computed from radar measures.

Most state-of-the-art image methods of nowcasting are based on a persistence assumption: a motion field is first estimated from the last two image acquisitions and further applied by a simulation model in order to synthetize images corresponding to the near future. In this applicative context, data assimilation methods, as defined in Bouttier et al. [2] and used in Ridal et al. [3], provide a framework for computing an optimal estimate of motion from a numerical model, composed of temporal evolution equations, and acquired observations, even if corrupted by noise. The nowcasting method that is described in this paper is based on two main components:

- a data assimilation method estimates the state of the system, including the wind field, based on the image acquisitions: this is the estimation phase.
- a forecast method uses this wind field estimation to extrapolate the state of the system in the future: this is the forecast phase that provides synthetic images of rainfall rates.

The notations and a description of the observations are given in Section 2. The assimilation process is summarized in Section 3, while the forecast and its results are described and displayed in Section 4.

2. CONTEXT AND NOTATIONS

The observations are acquired by a X band radar on a polar grid every five minutes. Angular resolution is one degree and radial resolution is 150 meters. The radial size is 240 pixels. A preprocessing is applied in order to obtain images of size 721×721 on a Cartesian grid of 100 meter resolution as shown on Fig. 1. The measured reflectivity Z is then transformed into a rainfall rate R, using the Marshal-Palmer [4]

*This research has been partially funded by the DGA.

Z-R relationship:

$$R = (\frac{1}{200} \times 10^{\frac{Z}{10}})^{\frac{5}{8}} \quad (1)$$

The studied system is characterized by a state vector $\mathbf{X}$, being composed of the two components u and v of motion $\mathbf{w}$ and of an image function I, which is defined at each location $(\mathbf{x}, t)$ of the studied space-time domain:

$$\mathbf{X}(\mathbf{x}, t) = \begin{pmatrix} u(\mathbf{x}, t) & v(\mathbf{x}, t) & I(\mathbf{x}, t) \end{pmatrix}^T \quad (2)$$

The temporal evolution of $\mathbf{X}$ satisfies a numerical model $\mathbb{M}$ with partial differential equations ruling the evolution of $\mathbf{w}$ and I with a time step dt. The image function I has physical properties similar to the input image observations $\mathbf{Y}$. These last are acquired with a temporal resolution Δt that is 5 minutes in this paper. In the following, temporal indexes (see Fig. 2) of the observations go from e_1 to e_K for the estimation phase that estimates the motion function. They are also computed every 5 minutes in the forecast phase and denoted f_1, f_2,...,f_i.

3. MOTION ESTIMATION FROM ASSIMILATION OF RADAR ACQUISITIONS

Operational constraints (being able to compute the motion fields in less than 2 minutes) force to reduce the temporal interval of acquisitions used for the estimation phase to 10 minutes (that corresponds to 3 consecutive image acquisitions) and to consider motion as stationary on that duration. The discrete evolution equations of the numerical model $\mathbb{M}$ are:

- Stationary motion:

$$\mathbf{w}(\mathbf{x}, t+1) = \mathbf{w}(\mathbf{x}, t) \quad (3)$$

- Transport of the image brightness by motion:

$$I(\mathbf{x}, t+1) = I(\mathbf{x}, t) - dt\,(\mathbf{w}(\mathbf{x}, t) \cdot \nabla I(\mathbf{x}, t)) \quad (4)$$

A semi-Lagrangian scheme is chosen as in Robert [5] for the integration in time of these two equations. Considering a pixel at position $\mathbf{x}$ and date t, whose velocity is $\mathbf{w}(\mathbf{x}, t)$ and brightness $I(\mathbf{x}, t)$, one has to compute $I(\mathbf{x}, t+1)$. For that, one should backtrack the trajectory arriving at $\mathbf{x}$ at $t+1$ in order to find its initial location $\mathbf{x} + \alpha$, where α corresponds to the displacement from t to $t+1$ and verifies:

$$\alpha = -dt \cdot \mathbf{w}(\mathbf{x}, t) \quad (5)$$

One may then define:

$$I(\mathbf{x}, t+1) = \mathcal{L}\,(I(\mathbf{x} + \alpha, t)) \quad (6)$$

with $\mathcal{L}\,()$ being the linear interpolation of the image brightness values for the pixels surrounding the location $\mathbf{x} + \alpha$. As shown in Pudykiewicz et al. [6], the use of linear interpolation is less accurate than higher order methods but still applied for satisfying the time constraints of operational use.

The adjoint of the numerical model $\mathbb{M}$, ruling the temporal evolution of $\mathbf{w}$ and I, is automatically computed by the differentiation software tapenade [7]. The operational version of the model $\mathbb{M}$ and of its adjoint are parallelized with OpenMP. A 4D-Var data assimilation method is then applied for estimating motion, similar to the one that is described in Bérézia t et al. [8] for the issue of motion estimation. It is based on an iterative minimization of a cost function, whose main term corresponds to the discrepancy between the actual observations $\mathbf{Y}(\mathbf{x}, e_i)$ and their equivalent in the state vector $I(\mathbf{x}, e_i)$. Motion is correctly estimated if these images approximately match: the transport of the image brightness $I(\mathbf{x}, t)$ by motion $\mathbf{w}(\mathbf{x}, t)$ is then similar to the observation $\mathbf{Y}$ at the acquisition dates.

Fig. 3 shows three consecutive observations that are assimilated with the numerical model $\mathbb{M}$ and allow to estimate the motion field displayed on the bottom-right, with a colored representation.

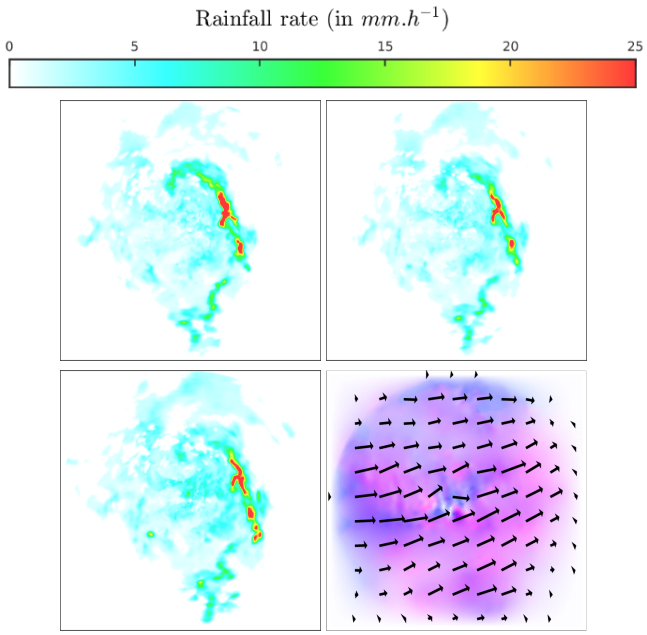

Fig. 3. Top to bottom and left to right: three observations and the estimated motion field.

4. NOWCASTING

The estimated motion field and the last acquired image are the inputs for the nowcasting phase. However, as the temporal horizon is at least 30 minutes, motion can no more be considered as stationary. The alternative, if not using NWP results, is to consider that the motion field is advected by itself. As

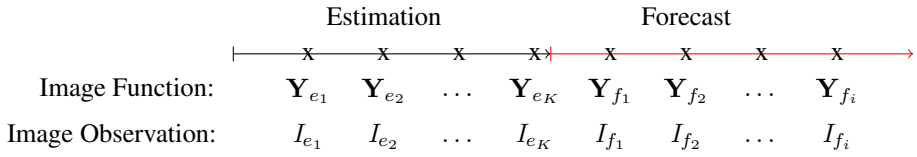

Fig. 2. Estimation and forecast phases.

the image brightness is still considered being transported by motion, the evolution equations of the state vector $\mathbf{X}(\mathbf{x},t)$ are:

$$\frac{\partial \mathbf{w}}{\partial t}(\mathbf{x},t) + (\mathbf{w}(\mathbf{x},t).\nabla)\mathbf{w}(\mathbf{x},t) = 0 \quad (7)$$

$$\frac{\partial I}{\partial t}(\mathbf{x},t) + \mathbf{w}(\mathbf{x},t)\cdot\nabla I(\mathbf{x},t) = 0 \quad (8)$$

Two spatial discretization schemes are at hand for the temporal integration.

1- A semi-Lagrangian scheme is unconditionally stable and allows a large time step, which decreases the number of integration steps (for the same simulation interval) and consequently the computational cost. However, if such time step has a value of several minutes, the trajectory of a pixel may no more being considered as linear. Let $\mathbf{x}$ be the position of a pixel. According to the evolution equations, the state vector value of $\mathbf{x}$ at time t is equal to its value at time $t-1$. However the location of $\mathbf{x}$ at time $t-1$ is unknown and must be computed. An equivalent alternative is to estimate the displacement from $t-1$ to t. This is obtained from the following process, described in Temperton et al. [9], with i being the iteration index. The total number of iterations is determined in advance. As the motion field is smooth in space, the angle of the tangent to the trajectory is also smooth and a small number of iterations is sufficient. The total number is then empirically given the value of 5.

$$\begin{aligned} \alpha_0 &= \frac{dt}{2}\left(3\mathbf{w}(\mathbf{x},t) - \mathbf{w}(\mathbf{x},t-1)\right) \quad (9)\\ &\dots \\ \alpha_{i+1} &= \frac{dt}{2}\left(2\mathbf{w}(\mathbf{x}+\alpha_i,t) - \mathbf{w}(\mathbf{x}+\alpha_i,t-1) + \mathbf{w}(\mathbf{x},t)\right) \end{aligned}$$

2- A Godunov scheme, solving Riemann problems at each inter-pixel boundary, is more accurate for advecting functions displaying high spatial gradient values. Such a scheme is fully described in in Béréziat et al. [8]. In this paper, the equations splitting method, described in Leveque [10], is also applied before discretization. However, beside the accuracy improvement, such an implementation imposes to satisfy the CFL conditions corresponding to the discretization schemes.

Consequently, our idea is to combine the two types of spatial discretizations in a mixed scheme, as summarized in Figure 4, so that the stability of the semi-Lagrangian scheme and the accuracy of the Godunov scheme both benefit the results. The Godunov scheme is first used for integrating $\mathbf{w}^G$ (G stands for Godunov) from the beginning of the forecast interval (that corresponds to the last date of the estimation phase, indexed by e_K) to the first acquisition (indexed by f_1. This Godunov motion value $\mathbf{w}^G(f_1)$ is then used by the semi-Lagragian scheme. For each pixel $\mathbf{x}$ at date f_1, its location $\mathbf{x}_{e_K}$ at date e_K is computed, thanks to the iterative technique described in Eq. 9, and the state vector value at location $\mathbf{x}_{e_K}$ is given to $\mathbf{x}$. This provides $\mathbf{w}^L(f_1)$ (L stands for Lagrangian) and the reflectivity forecast $I(f_1)$. The process is further iterated until the second acquisition by initializing the Godunov scheme with the semi-Lagrangian value $\mathbf{w}^L(f_1)$, and so on. For practical use, the time step of the Godunov scheme is 1 second and the one of the semi-Lagrangian scheme is 5 minutes.

Results of nowcasting are easier to analyze if quantified as rainfall quantities, which are cumulated rainfall rates on given durations from 15 minutes to 1 hour, and compared to the observed rainfall quantities, as displayed on Fig. 5 for 30 minutes. Results can then be assessed by comparing the

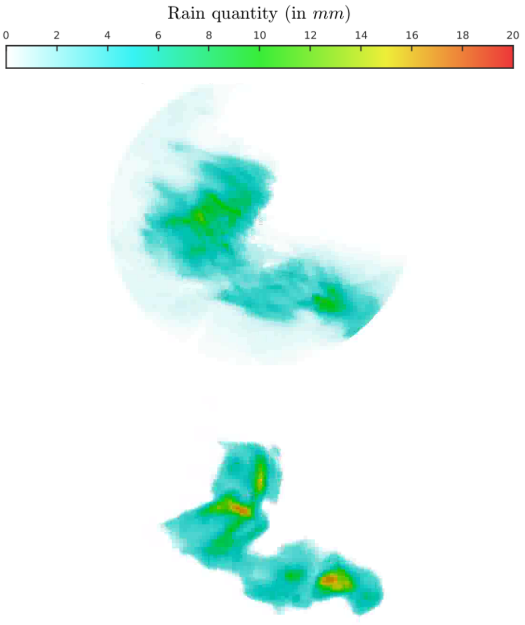

Fig. 5. Top: observed cumulated rainfall quantity over 30 minutes. Bottom: nowcasting result. Copyright Numtech.

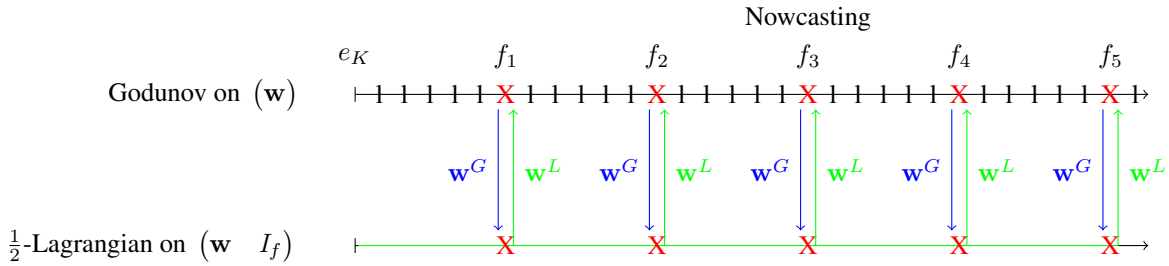

Fig. 4. Schematic representation of the mixed model.

locations of alerts of heavy rain, obtained by thresholding the nowcasted values, with the effective ones. This information, required by decision makers for implementing prevention measures, is computed on space-time neighborhoods as emergency measures are taken at regional level. In that context, the percentage of sent alerts actually measured is of 90% at one hour. However, due to the nature of the model that only considers advection processes, the percentage of measured alert actually forecasted is 66% at a 15 minutes horizon and falls to 58% at one hour.

5. CONCLUSION

The paper describes a method for nowcasting rain at short temporal horizon from image data acquired at high resolution and high temporal frequency by ground radars. The method is based on a motion estimation component and on a simulation tool.

The approach allows to provide alert of flash floods, accordingly with the time scale of image acquisitions, and a number of perspective has been defined for improving the forecast results. First, processes should be rewritten in polar coordinates, according to the acquisition process, for avoiding preprocessing. Second, an object component will be added to the state vector in order to get an improved motion estimation and a better localization of endangered regions. Last, nowcasting will be improved by combining with outputs of Numerical Weather Prediction models in order to allow long-term forecasts.

Acknowledgements

The authors acknowledge the company Weather Measures for providing data from its radars and the company Numtech for the implementation of the method in an operational context and the visualizations included in the paper.

6. REFERENCES

[1] S. Mecklenburg, A. Jurczyk, J. Szturc, and K Osrodka, "Quantitative precipitation forecasts (QPF) based on radar data for hydrological models," in *COST action*, 2002.

[2] F. Bouttier and P. Courtier, "Data assimilation concepts and methods," Tech. Rep., Training Course of European Centre for Medium-Range Weather Forecasts, 1999.

[3] M. Ridal, M. Lindskog, N. Gustafsson, and G. Haase, "Optimized advection of radar reflectivities," *Atmospheric Research*, 2011.

[4] John S Marshall and W Mc K Palmer, "The distribution of raindrops with size," *Journal of meteorology*, 1948.

[5] A. Robert, "A stable numerical integration scheme for the primitive meteorological equations," *Atmosphere-Ocean*, 1981.

[6] J Pudykiewicz and A Staniforth, "Some properties and comparative performance of the semi-lagrangian method of robert in the solution of the advection-diffusion equation," *Atmosphere-Ocean*, 1984.

[7] L. Hascoët and V. Pascual, "Tapenade 2.1 user's guide," Tech. Rep., INRIA, 2004.

[8] D. Béréziat and I. Herlin, "Solving ill-posed image processing problems using data assimilation," *Numerical Algorithms*, 2011.

[9] C. Temperton, M. Hortal, and A. Simmons, "A two-time-level semi-Lagrangian global spectral model," *Quarterly Journal of the Royal Meteorological Society*, 2001.

[10] R. LeVeque, *Numerical Methods for Conservative Laws*, ETH Zürich, Birkhaüser Verlag, 1992.